



Optics Letters

Fourier transform spectroscopy by repetition rate sweeping of a single electro-optic frequency comb

M. IMRUL KAYES* AND MARTIN ROCHETTE

Department of ECE, McGill University, 3480 University Street, Montreal, Québec H3A 0E9, Canada

*Corresponding author: imrul.kayes@mail.mcgill.ca

Received 16 November 2017; revised 7 January 2018; accepted 7 January 2018; posted 16 January 2018 (Doc. ID 313566); published 16 February 2018

We demonstrate the operation of a Fourier transform spectrometer that operates by sweeping the pulse repetition frequency of an electro-optic frequency comb. Incorporating a length-imbalanced interferometer, this single-comb system is analogous to a conventional dual-comb system, but with a greatly simplified design. The functionality of the spectrometer is demonstrated via the high-resolution spectrum measurement of an $\text{H}^{13}\text{C}^{14}\text{N}$ reference gas cell. © 2018

Optical Society of America

OCIS codes: (300.6300) Spectroscopy, Fourier transforms; (230.2090) Electro-optical devices; (060.3510) Lasers, fiber.

<https://doi.org/10.1364/OL.43.000967>

Optical frequency combs (OFCs) are made of mutually coherent, narrow, and equally spaced spectral lines. Phase matching across the spectral lines of a frequency comb is appealing for numerous applications such as coherent optical communication, arbitrary waveform generation, low noise microwave generation, and most importantly, spectroscopy [1,2]. Especially for broadband molecular spectroscopy, the hundreds to thousands of sharp spectral lines make the OFC a suitable tool for spectrum sensing with high resolution and high sensitivity [3]. However, to detail individual spectral lines, an optical spectrum analyzer with a resolution as high as the spectral lines under investigation must be used, which is typically expensive, if available. In the case of traditional Fourier transform (FT) spectrometers, comb sources can replace incoherent light sources to offer an improved signal-to-noise ratio. However, comb sources do not overcome the two disadvantages of FT spectroscopy, which are the requirement of a mechanical scan mirror and an output resolution that is limited by the maximum path difference between two interferometric arms.

In response to this, dual-comb spectroscopy overcomes these limitations by employing two combs of slightly different repetition rates and produces a cross-correlational interferogram at the sample [4]. This method has ultrafast acquisition time, no moving parts, and a resolution determined by the repetition frequency of the comb. However, the strict phase-matching requirements between both combs make this system complex, bulky, and not suitable for field use.

Single-comb spectroscopy with a sweeping repetition frequency is a simple and efficient alternative to the ones presented above [5]. It uses a length-imbalanced interferometer to create two pulse trains of different instantaneous frequencies. Optical path delays between two overlapping pulse pairs are scanned by changing the repetition frequency (f_r) of the comb. Since one arm of the interferometer is shorter than the other, a change of the repetition frequency impacts the output of the shorter arm at first, and momentarily two pulse trains with different repetition frequencies are generated. The system becomes analogous to a dual-comb system when the repetition frequency is varied continuously. After a complete scan of the repetition frequency, a recorded cross-correlational interferogram is produced at the photodetector. This method is also known as optical sampling by laser cavity tuning (OSCAT), first proposed in Ref. [6]. As the name suggests, this method was originally intended for mode-locked laser (MLL)-based OFC where f_r sweeping is achieved by means of varying the laser cavity length with a piezoelectric actuator. However, the dynamic range of such f_r sweeping is limited due to stabilization constraints of the MLL cavity. As a result, one needs a long (>200 m) delay line to achieve sufficient spectral resolution for spectroscopy. A long delay line is sensitive to ambient temperature variation and causes interferometric timing and phase fluctuation of the comb signal [5,7]. To compensate for the impairments of the delay line, two narrow bandpass filters must be used to track the timing and phase variation. By extracting the phases of the filtered signal, the phase and timing grid of the interferogram are corrected [8].

Electro-optic (EO)-comb-based dual-comb systems have greatly improved in the last few years [9–11]. Effectively, dual EO combs are seeded from one continuous-wave (CW) laser. This brings the main benefit of EO combs, which is that, in contrast to mode-locked-based systems, EO combs do not require phase matching. However, for the optical bandwidth of EO combs to cover hundreds of nanometers (nm), multiple sections of pulse compression, amplification, and nonlinear mixing are required, often via adding kilometer (km)-long optical fibers. Maintaining the coherence of two EO combs over such a long length of fiber is a challenging task, degrading the performance of dual-comb EO systems. In contrast, single-EO-comb-based systems are coherence independent and thus

more suitable for spectroscopy with an ultra-wide optical bandwidth (>150 nm) [12]. Also, in terms of signal-to-noise ratio (SNR), single-comb systems perform better than dual-comb systems. For dual-comb systems, each interferogram must cover the complete optical path length difference set by the difference in repetition rate. For single-comb systems, periodic variation in repetition frequency means that a small and selectable pulse detuning range can be covered, and this translates into an improved SNR since all pulses are probing a specific spectral range of interest [8]. It is only in terms of acquisition speed that dual-comb systems outperform single-comb-based systems, since the acquisition speed of a dual-comb system is limited by the bandwidth of its detector (\sim ms), whereas the acquisition speed in a single-comb system is limited by the tuning speed of its microwave source (\sim s).

In this Letter, we demonstrate the operation of a single-EO-comb-based spectrometer (SCS) that operates by repetition frequency sweeping. The SCS overcomes the limitations of mode-locked-laser-based systems, bypassing the phase correction requirement by offering greater dynamic range of repetition frequency sweeping. Greater dynamic range mitigates the delay length requirement for maximum resolution and minimizes the interferometric phase fluctuation. Moreover, this approach offers long-term stability since there is no cavity involved in the EO comb generation process [13]. In comparison with the so-called optical vector network analyzer technique [14], the SCS is faster and capable of covering a broader spectrum. This is because the SCS can probe simultaneously the entire band covered by its comb lines, whereas the optical vector network analyzer probes only in the vicinity of the CW laser line.

An OSCAT system mimics a dual-comb system by using a periodic variation of the pulse repetition rate transmitted through an imbalanced interferometer. Due to a pulse buffer effect on one interferometer's arms, a variation of the pulse repetition rate is transmitted through the shorter arm first, then through the longer arm second, with a delay that corresponds to the difference in the arms' lengths. Two pulse trains with different repetition rates thus reach the output of the interferometer and superimpose for a brief period of time. The OSCAT system becomes completed with a smooth and cyclic variation of the comb repetition rate, resulting in a variation of the relative delay in between pulses coming from each interferometer's arm and thus forming an interferogram at detection.

Next, we derive the relative time delay between a pulse pair for each incremental change in comb repetition frequency [5]. If L is the length mismatch between two arms, then the number of pulses stored in the delay fiber is given by $N = L \cdot f_r \cdot n/c$, where c is the speed of light in a vacuum and n is the group refractive index of the fiber. The repetition frequency at the peak position of the interferogram determines f_r . The time delay that separates a pulse and its delayed version after passing through the interferometer (pulse pair) is $\tau = L \cdot n/c = N/f_r$. Thus, for each incremental change δf_r of repetition frequency, the resulting increment in time delay for the pulse pair is

$$\delta\tau = -N \cdot \frac{\delta f_r}{f_r^2}.$$

The maximum optical path delay of the pulse pair after a full f_r scan is given by $\text{MPD} = \delta\tau \cdot n_{\text{step}} = -N \cdot \delta f_r \cdot n_{\text{step}}/f_r^2$, where n_{step} is the number of frequency scan steps. The spectral resolution (R) is given by $R = \max(f_r, \text{MPD}^{-1})$ and determined by the inverse of MPD if not limited by repetition

rate [8]. Thus, we conclude that increasing the product $N \cdot \delta f_r \cdot n_{\text{step}}$ maximizes spectral resolution. In the case of a MLL-based comb, the dynamic range of f_r sweeping is limited. Therefore, the only way for MLL-based combs to maximize resolution is to increase N or L . This has been done in previous works using the OSCAT method [4,6,11]. The main drawback of this approach is the requirement of a long delay fiber that imposes phase and timing variation between pulse pairs, which subsequently needs to be corrected using two reference fiber Bragg gratings (FBGs) [8]. On the other hand, the use of an EO comb increases the dynamic range (δf_r) in sweeping pulse repetition rate and thus achieves high resolution from a short delay fiber (<15 m). The spectral resolution of such method is determined by the comb repetition frequency, the acquisition time is determined by the scan speed of the repetition rate sweeping mechanism, and the absolute wavelength accuracy of the Fourier spectrum is determined by the uncertainty of the carrier wavelength.

Figure 1 shows the experimental implementation of the SCS. An EO comb is generated by phase modulation, chirp compression, and nonlinear mixing of a CW signal at a wavelength of 1540 nm [15]. The EO comb consists of a pulse train with a repetition frequency of ~ 10 GHz. The pulse width is 10 ps, and its spectral full width at 10 dB from the maximum is 30 nm with an optical SNR >20 dB throughout.

Figure 2 shows the spectrum of the resulting OFC. The repetition frequency is controlled by the sinusoidal signal of a radio frequency (RF) clock generator, and can be tuned over the 9–11 GHz range without significant change in optical bandwidth. A tunable bandpass filter truncates half of the optical spectrum from 1522 nm up to 1537 nm to prevent aliasing of spectroscopic measurement. Bandpass filtering would be unnecessary if an acousto-optic modulator was used in one arm, resulting in a twofold increase in the effective bandwidth, as is the case for EO dual-comb systems [10,11]. The filtered OFC signal is then sent to an imbalanced Mach-Zehnder interferometer (MZI). A polarization controller is used in one arm to maximize the beating signal amplitude at the output

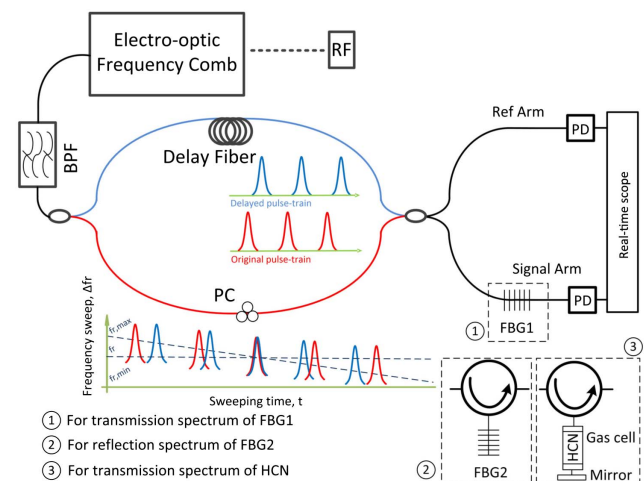


Fig. 1. Experimental setup to demonstrate the concept of single-comb spectroscopy with sweeping pulse repetition rate. Three samples are shown in the dashed boxes (FBGs and an $\text{H}^{13}\text{C}^{14}\text{N}$ gas cell) and numbered in accordance with the order of their presence in the Letter. BPF: bandpass filter; PC: polarization controller; FBG: fiber Bragg grating; PD: photodiode.

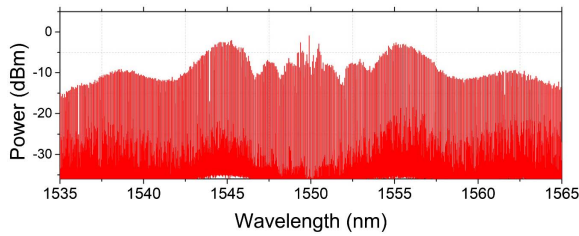


Fig. 2. Spectrum of the 10 GHz EO frequency comb.

of the MZI. The net physical length difference in between the MZI's arms is provided by an optical fiber with a length of 12.15 m. After passing through the MZI, the resulting interferometric signal is divided in two halves, where one half is passed through the signal arm containing a spectroscopic sample to analyze, detected with a 100 MHz photodiode, and recorded with a real-time oscilloscope of 1 GSa/s bandwidth. The other half of the interferometric signal is passed through the reference arm and detected by another photodiode to record the signal simultaneously without the sample.

The first analyzed sample is a fiber Bragg grating (FBG1) having a central wavelength of 1529.37 nm, a full width at half-maximum (FWHM) of 0.2 nm, and transmission depth of ~ 9 dB. The RF signal is swept from 10.010 to 10.035 GHz in 1000 steps with a frequency step size of 25 kHz. At each frequency step, the oscilloscope records the optical power from the MZI output after passing through the sample. It forms an interferogram signal at the oscilloscope after one full scan, containing the transmission spectrum of the sample under test. Signal from the reference arm is also recorded at the oscilloscope simultaneously.

The second sample is FBG2, working in the reflection mode thanks to a circulator. FBG2 has a central wavelength of 1529.33 nm, a FWHM of 0.3 nm, and transmission depth of ~ 20 dB. After sweeping the RF signal, interferograms from both signal and reference arm are recorded by the oscilloscope.

The proposed spectroscopic system is also used to measure the transmission spectrum of an $\text{H}^{13}\text{C}^{14}\text{N}$ reference gas cell. For this purpose, a 16.5 cm long $\text{H}^{13}\text{C}^{14}\text{N}$ gas cell with a pressure of 25 Torr is inserted in the signal arm. A circulator and a fiber mirror are used for the incoming light to perform a double pass in the gas cell for increased sensitivity. Since each absorption line of $\text{H}^{13}\text{C}^{14}\text{N}$ has a FWHM ~ 2 GHz, the repetition frequency of the reference RF clock is reduced to 2 GHz and swept from 2.010 to 2.050 GHz with a frequency step of 40 kHz. In this process, the total optical bandwidth becomes reduced with respect to the configuration used to analyze the FBGs, resulting in an effective bandwidth of 1 nm after bandpass filtering. The central wavelength of the comb is shifted a number of times to cover 8 nm of spectral bandwidth, as explained in a later paragraph.

Figure 3 shows interferograms for both FBG samples. Figure 3(a) shows the periodic interferogram recorded by an oscilloscope after passing through FBG1 in red and FBG2 in blue. The acquisition speed per interferogram is 4 s, which can be substantially reduced by optimizing the number of frequency scan steps. The acquired interferogram is low-pass filtered to filter out the noisy fluctuations by sampling at the effective time step calculated from Eq. (1). This is performed in MATLAB, using a moving average filter with a relative cutoff frequency of 0.2. The interferogram is subsequently zero-padded to smooth out the peaks in the spectrum and

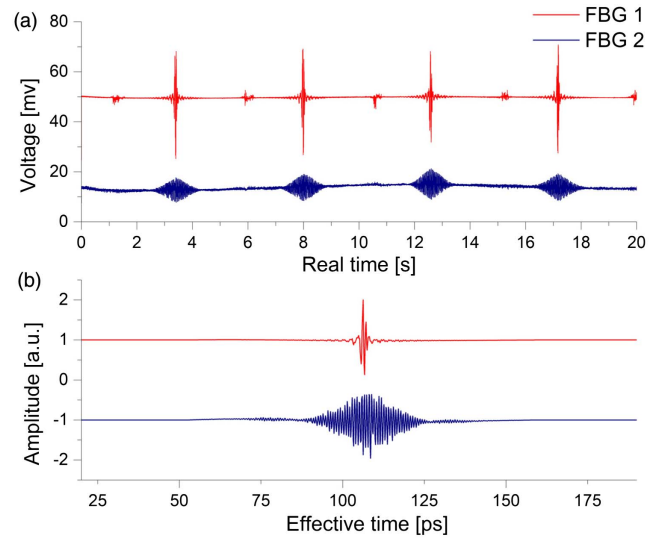


Fig. 3. (a) Periodic interferogram recorded in oscilloscope after both sample FBG1 and FBG2. (b) Interferogram after low-pass filtering, apodization, and zero-padding.

apodized by multiplying with a triangular signal to minimize the oscillations of the spectral envelope. The resulting post-processed interferogram is shown in Fig. 3(b). The post-processed interferograms are Fourier transformed to obtain the spectral response of the samples. The spectrum resolution is set by the 10 GHz repetition frequency of the comb, which is fine enough to resolve the spectral signature of the FBG samples. This resolution is better than some dual-comb counterparts, reporting a measurement resolution of ≥ 20 GHz [11,16].

Figure 4 shows the retrieved spectra of FBG1 and FBG2. Figure 4(a) shows the total power transmitted by FBG1 and reflected by FBG2. The spectrum profile of FBG1 originates from the OFC envelope after bandpass filtering. The dip at a wavelength of 1529.37 nm with a depth of ~ 9 dB fits well with

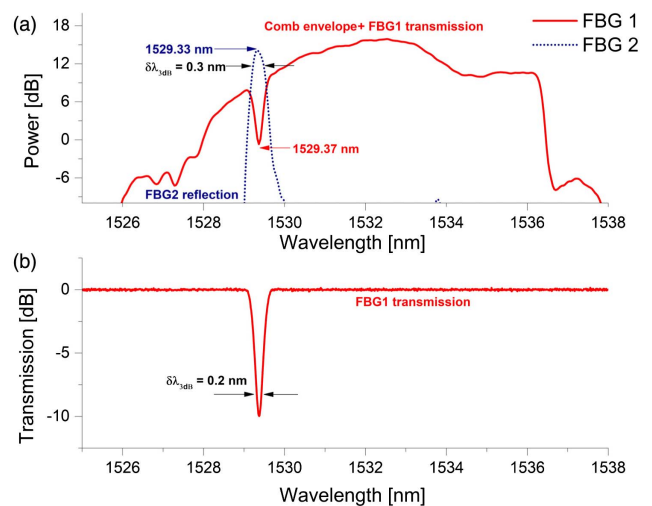


Fig. 4. (a) Resulting spectra after Fourier transforming the interferograms from Fig. 3(b). FBG1 operates in transmission mode, while FBG2 operates in reflection mode. (b) Transmission spectrum of FBG1 is retrieved after subtracting the spectrum of the reference arm from the spectrum of the signal arm.

the expected transmission spectrum of FBG1. Multi-path interference produces small ripples observed on the spectrum, but is accounted for by subtracting a reference spectrum without any sample present. Figure 4(b) shows the transmission spectrum of FBG1, as retrieved after subtracting a reference spectrum. The reflectance spectrum of the reference FBG2 is also provided on Fig. 4(a) with a peak at 1529.33 nm. Both center wavelengths and FWHM match well the values obtained with a high-resolution optical spectrum analyzer (*Yokogawa*), with an absolute wavelength accuracy of ± 0.01 nm.

The calculated spectra are retrieved from a single interferogram without averaging. However, coherent averaging may be used to enhance the SNR of the interferogram. The SNR increases with the square root of the number of averaged spectra (N_a). To measure the SNR, we consider 10 Fourier spectra to measure the normalized standard deviation of the amplitude noise. The frequency domain SNR is the inverse of the standard deviation and calculated to be $\text{SNR} = 50$ for 10 averaged spectra over 15 nm of optical bandwidth (BW). The highest reported SNR for an EO dual-comb system was 2500 for 100 averaged spectra over a bandwidth of 0.5 nm [10]. When comparing the figure of merit ($\text{SNR} * \text{BW} / \sqrt{N_a}$), the SCS method has almost twice the value. However, the acquisition speed of the dual-comb method is 1 ms, that is, faster than the SCS method. The measurement accuracy of the wavelengths is dependent on the absolute wavelength accuracy of the carrier signal of the OFC. To increase the spectral resolution of measurement, one has to use a comb with lower repetition frequency, since resolution of such a system is ultimately limited by its repetition rate. However, a smaller frequency spacing comes with a smaller bandwidth, leading to a trade-off between spectral resolution and spectral range.

For the transmission spectrum analysis of the $\text{H}^{13}\text{C}^{14}\text{N}$ gas cell, the comb repetition frequency is set to ~ 2 GHz, as required by the resolution of the transmission features of the sample. However, this leads to an optical bandwidth of 2 nm. To increase the wavelength range, that is, measuring the R2–R14 absorption lines of $\text{H}^{13}\text{C}^{14}\text{N}$ covering 1533–1541 nm, the carrier frequency of the OFC is shifted once every ~ 0.75 nm. In each section, four interferograms are coherently averaged to produce

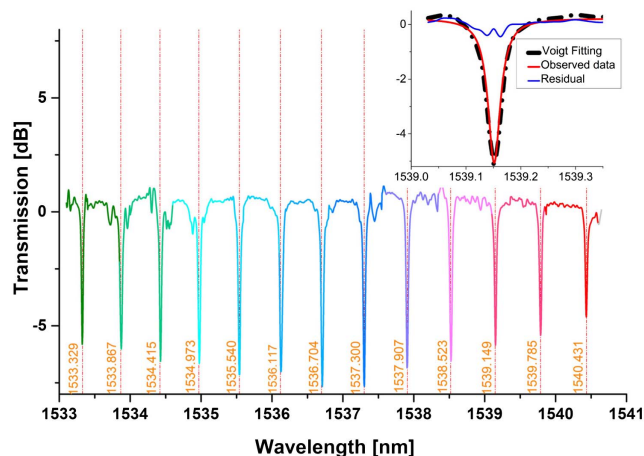


Fig. 5. Transmission spectrum of the $\text{H}^{13}\text{C}^{14}\text{N}$ gas cell showing the absorption lines between R2–R14 branches. The vertical lines denote the true absorption wavelength value for each branch as per the NIST test data. The inset shows the Voigt fitting of the R4 branch.

the final interferograms for both signal and reference arms. This pair of interferograms are then Fourier transformed to produce the corresponding spectra. The reference spectrum is subtracted from the signal spectrum to obtain the transmission spectrum for one section. All of the sections are then combined together after averaging the overlapping sections to obtain the complete transmission spectrum of the gas cell. Figure 5 shows the resulting transmission spectrum of the R2–R14 branches of $\text{H}^{13}\text{C}^{14}\text{N}$. The relative amplitude of the 13 transmission dips matches the transmission spectrum of the reference gas cell's datasheet [17]. After getting the transmission spectrum, the peak absorption wavelengths measured in the experiment are compared against their National Institute of Standards and Technology's (NIST) standard values. The experimental versus reference spectra differ by a maximum of ± 9 pm. This discrepancy is attributed to the absolute wavelength accuracy of ± 10 pm of the tunable laser that seeds the OFC. Thus, it can be assumed that with a precise measurement of carrier wavelength within ± 1 pm, the measured value will match the NIST standards within an accuracy of < 1 part per million.

In summary, we have shown that a spectrometer based on a single EO comb and a length-imbalanced MZI successfully and accurately determines the spectral response of a chemical sample. Since it only uses one comb source, the system does not need to satisfy any strict phase-matching criterion. The use of one EO comb and a short length (~ 12 m) of delay fiber enable this measurement and bypass the requirement of two-reference phase correction. EO combs are more flexible than MLLs in terms of tunability of the comb repetition rate and long-term stability in field deployment, which constitutes an advantage for comb-based spectroscopy. Unlike MLL-based systems, the resolution of an EO comb and length-imbalanced MZI system is not limited by the maximum path delay, but rather by the comb repetition rate, like a dual-comb spectrometer.

REFERENCES

1. S. A. Diddams, *J. Opt. Soc. Am. B* **27**, B51 (2010).
2. I. Coddington, N. Newbury, and W. Swann, *Optica* **3**, 414 (2016).
3. S. A. Diddams, L. Hollberg, and V. Mbele, *Nature* **445**, 627 (2007).
4. T. Ideguchi, A. Poisson, G. Guelachvili, N. Picqué, and T. W. Hänsch, *Nat. Commun.* **5**, 21932 (2014).
5. K. Lee, J. Lee, Y.-S. Jang, S. Han, H. Jang, Y.-J. Kim, and S.-W. Kim, *Sci. Rep.* **5**, 15726 (2015).
6. T. Hochrein, R. Wilk, M. Mei, R. Holzwarth, N. Krumbholz, and M. Koch, *Opt. Express* **18**, 1613 (2010).
7. C. Mohr, A. Romann, A. Ruehl, I. Hartl, and M. E. Fermann, *Advances in Optical Materials*, OSA Technical Digest (CD) (OSA, 2011), paper FWA2.
8. S. Potvin, S. Boudreau, J.-D. Deschênes, and J. Genest, *Appl. Opt.* **52**, 248 (2013).
9. A. J. Fleisher, D. A. Long, Z. D. Reed, J. T. Hodges, and D. F. Plusquellic, *Opt. Express* **24**, 10424 (2016).
10. G. Millot, S. Pitois, M. Yan, T. Hovhannisyann, A. Bendahmane, T. W. Hänsch, and N. Picqué, *Nat. Photonics* **10**, 27 (2016).
11. V. Durán, P. A. Andrekson, and V. Torres-Company, *Opt. Lett.* **41**, 4190 (2016).
12. E. Myslivets, B. P. P. Kuo, N. Alic, and S. Radic, *Opt. Express* **20**, 3331 (2012).
13. M. I. Kayes and M. Rochette, *Photonics North (PN)* (IEEE, 2016), paper Nonlinear-10-6.
14. J. E. Román, M. Y. Frankel, and R. D. Esman, *Opt. Lett.* **23**, 939 (1998).
15. M. Imrul Kayes and M. Rochette, *Opt. Lett.* **42**, 2718 (2017).
16. P. Martín-Mateos, B. Jerez, and P. Acedo, *Opt. Express* **23**, 21149 (2015).
17. "Wavelength References," <https://goo.gl/AHnFMp>.